Progress In Electromagnetics Research B, Vol. 52, 207–236, 2013

COMPACT-LIKE PULSE SIGNALS IN A NEW NONLINEAR ELECTRICAL TRANSMISSION LINE

Désiré Ndjanfang[1], David Yemélé[2, *], Patrick Marquié[3], and Timoléon C. Kofané[1]

[1]Laboratoire de Mécanique, Faculté des Sciences, Université de Yaoundé I, B.P. 812, Yaoundé, Cameroun

[2]Laboratoire de Mécanique et de Modélisation des Systèmes Physiques L2MSP, Faculté des Sciences, Université de Dschang, B.P. 067, Dschang, Cameroun

[3]Le2i, Université de Bourgogne, UMR CNRS 5158, Ailes Sciences de l'Ingénieur, Boite Postale 47870, Dijon Cedex 21078, France

Abstract—A nonlinear electrical transmission line with an intersite circuit element acting as a nonlinear resistance is introduced and investigated. In the continuum limit, the dynamics of localized signals is described by a nonlinear evolution equation belonging to the family of nonlinear diffusive Burgers' equations. This equation admits compact pulse solutions and shares some symmetry properties with the Rosenau-Hyman $K(2,2)$ equation. An exact discrete compactly-supported signal voltage is found for the network and the dissipative effects on the pulse motion analytically studied. Numerical simulations confirm the validity of analytical results and the robustness of these compact pulse signals which may have important applications in signal processing systems.

1. INTRODUCTION

Dispersive nonlinear systems have received a renewal of attraction since the pioneering work by Rosenau and Hyman [1] introducing the concept of solitary waves with compact support and compactons. In fact, as pointed out by these authors, unlike standard solitary waves which in spite of being localized, extend indefinitely [2], compact solitary waves have a finite extension, that is, they vanish identically

Received 2 March 2013, Accepted 10 May 2013, Scheduled 6 June 2013

* Corresponding author: David Yemélé (dyemele@yahoo.fr).

outside a finite region in space, and this results from the delicate balance between nonlinear dispersion and standard nonlinearity of the system. After this pioneering work, many studies appeared with the goal to a deeper understanding of the mechanism at the basis of this phenomenon and demonstrated that compact waves may also emerge in a variety of physical contexts and that, its mathematical characterization is universal and given via a sub-linear substrate potential or on-site force, a nonlinear diffusion, a sub-linear convective, to cite just a few. The common mathematical thread of these diverse phenomena is the degeneracy of differential equations describing their properties at certain points and the corresponding failure of the uniqueless theorem at these. In this respect, one can quote the compactification of nonlinear patterns and waves by Rosenau and Kashdan [3], Weierstrass criterion and compact solitary waves by Destrade et al. [4], compact solitary waves in linearly elastic chain with non-smooth on-site potential by Gaeta et al. [5], and on compactification of patterns by a singular convection or stress by Rosenau [6].

In order to put forward this new concept on one hand and to improve the understanding of some physical phenomena on the other, many other works appearing in the literature deal with the theory and the possible relevance of compact solitary waves for applications. For example, Kivshar [7] reported that intrinsic localized modes in purely anharmonic lattices may exhibit compactons like properties while Kevrekidis et al. [8] demonstrated that discrete compactons cannot travel. Similarly, Dusuel et al. [9] demonstrated that the same phenomelogy can also appear in nonlinear Klein-Gordon systems with anharmonic coupling, and then obtained the experimental evidence of the existence of the static kink compactons in a real system made up by identical pendulums connected by anharmonic springs. We may also mention the analysis of patterns on liquid surfaces [10], the nonlinear dynamics of surface internal waves in a stratified ocean under the Earth's rotation [11], the modelling of DNA opening with 1D Hamiltonian lattice [12], the dynamics of a chain of autonomous, self-sustained, dispersively coupled oscillators [13, 14], the motion of melt in the Earth [15, 16]; all these studies were performed by means of the compacton concept, to cite just a few. In systems where the compactification of wave results from the non-smoothing of the on-site potential, some different features absent in the original system characterized by the nonlinear dispersion arise, namely, the possibility of a wave with compact support to propagate with arbitrary velocity [3, 5].

Another interesting issue for such structures is whether they

can be supported by signal processing tools such as nonlinear electrical transmission lines (NLTLs). The development in NLTLs has demonstrated its capacity to work as signal processing tools [2, 17]. To cite only a few examples, it has been demonstrated that the nonlinear uniform electrical line can be used: for extremely wide band signal shaping applications [18], for waveform equalizer in the compensation scheme for signal distortion caused by optical fibre polarisation dispersion mode [19], for doubling repetition rate of incident pulse streams [20] and in the scheme for controlling the amplitude (amplification) and the delay of ultra-short pulses through the coupled propagation of the solitonic and dispersive parts, which is important in that it enables the characterization of high-speed electronic devices and raises the possibility of establishing future ultra-high signal processing technology [21]. So, the emergence of compactons in nonlinear lattices can be a spring towards the important improvement of practical results concerning the distortion-less signal in ultrahigh-speed signal processing tools and in electronic devices where they may be used to codify data. In this spirit, Comte and Marquié [22] pointed out that the introduction of the nonlinear resistance in the series branch of the nonlinear transmission line modeling the front propagation in reaction-diffusion equations can create a nonlinear diffusion and then the compactification of kink solitary waves. Similarly, Yemélé and Kenmogné [23, 24] demonstrated that, if the NLTL is built conveniently, it may also exhibit dynamics compact envelope dark solitary waves while English et al. [25] demonstrated that very narrow intrinsic localized modes can also exist in the discrete NLTL with inter-site nonlinearities with the speed quite sensitive to the ratio of intensity to on-site nonlinearities.

Our purpose in this paper is to show that compact-like electrical pulse signals can propagate in the NLTL with well-defined basic characteristics and in the continuum limit. To this end, the work is organized as follows: In Section 2, we present the characteristics of the NLTL under consideration and derive the circuit's equations governing the dynamics of signal voltage in the network. In Section 3, we show that these equations may be reduced to a nonlinear evolution equation belonging to the family of nonlinear diffusive Burgers' equations which admits a pulse solitary wave with compact support as a solution. Next, exact discrete solution of the network is derived in Section 4. In Section 5, by means of a simple perturbation theory, we investigate dissipation effects of the network components on the compact pulse motion. Numerical investigations and simulations are carried out in Section 6 in order to check the validity of the analytical predictions. Finally, Section 7 is devoted to concluding remarks.

2. MODEL DESCRIPTION

We consider a lumped nonlinear transmission line which consists of a number of cells connected as illustrated in Figure 1. Each cell contains in the series branch a linear inductor L shunted by a nonlinear resistance (NLR) and in the shunt branch the well-known bias-dependent capacitor $C(V)$ responsible for the standard nonlinearity of the network. Its capacitance is assumed to be expanded as a power series of the local signal voltage V_n, which appears across the nonlinear capacitor of the nth cell:

$$\frac{dq_n}{dV_n} \equiv C(V_b + V_n) = C_0 \times (1 - 2\alpha V_n)\,, \tag{1}$$

where $C_0 \equiv C(V_b)$ is a constant corresponding to the capacitance of the nonlinear capacitor at the dc bias voltage V_b, and $\alpha \equiv -C'(V_b)/2C(V_b)$ is a parameter characterizing the nonlinearity while q_n is the electrical charge stored in the nth capacitor. From Kirchhoff's laws, the circuit equations for the line are given by:

$$\begin{aligned} V_{n-1} - V_n &= L\frac{di_n^L}{dt}, \\ \frac{dq_n}{dt} &= i_n - i_{n+1}, \\ i_n &= i_n^L + i_n^{\mathrm{NLR}}, \end{aligned} \tag{2}$$

where i_n^{NLR} and i_n^L are the currents passing through the NLR and the linear inductor L, respectively.

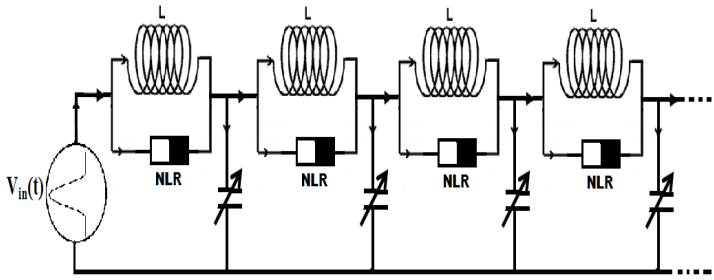

Figure 1. Schematic representation of the lumped nonlinear transmission line under consideration. Each cell contains the nonlinear capacitor $C(V)$ in the shunt branch which induces the standard nonlinearity, the linear inductor L and the Nonlinear Resistance (NLR) introducing the linear dispersion and nonlinear diffusion, respectively, in the network.

In order to build the circuit that can allow the propagation of compactly supported electrical signals, it is important to choose the NLR properly which can create the appropriate nonlinearity responsible for the compactification of pulse signal voltages in the network. Works on this issue were first made by Comte and Marquié [22]. If the NLR is replaced by a nonlinear capacitor, it is then possible to obtain modulated gray and dark compactons [23]. Unfortunately, neither this nonlinear capacitor nor the NLR with cubic nonlinearity introduced by Comte and Marquié [22] to compactify kink solitons may be used to create compact electrical pulse signal in the NLTL. In this paper we consider the NLR with the following current-voltage characteristics:

$$i_n^{\mathrm{NLR}} = a\delta V_n + b(\delta V_n)^2, \tag{3}$$

where a is a constant parameter describing the linear or first order conductance while the parameter b stands for the second order conductance. In the context of the NLTLs, a also describes either the linear dissipation ($a > 0$) or the energy pump ($a < 0$) in the network, b a parameter that controls the strength of the nonlinearity while $\delta V_n = V_{n-1} - V_n$ is the voltage across the NLR. Let us mention that the NLR was introduced recently in NLTL for signal processing applications and more precisely for nonlinear filtering of images [26, 27], noise removal on coherent information weakly varying in space, signal amplification and for modulational instability [28, 29]. This NLR may be made of operational amplifiers, transistors, or multipliers [30]. More interestingly, the NLR described by Equation (3) may be viewed also as a second order approximation of the current-voltage characteristics of the standard diode, $i_n = i_0[\exp(e\delta V_n/k_BT) - 1]$, provided a and b are positive constants. Accordingly, the case $a = 0$ gives rise to the well-known current voltage characteristics of the quadratic diode operating in the forward bias regime. In the following, we first consider this latter case and the influence of the linear term will be considered later.

With the above defined characteristics, Equations (1) to (3) can then be rewritten and combined into the following set of differential equations governing signal propagation in the network:

$$\begin{aligned} &\frac{d^2V_n}{dt^2} + \omega_0^2\left(2V_n - V_{n-1} - V_{n+1}\right) \\ =\ &\alpha\frac{d^2V_n^2}{dt^2} - \gamma\frac{d}{dt}\left[\left(V_n - V_{n+1}\right)^2 - \left(V_{n-1} - V_n\right)^2\right] \end{aligned} \tag{4}$$

with

$$\gamma = b/C_0, \quad \omega_0^2 = 1/LC_0, \tag{5}$$

and for $n = 1, 2, \ldots, N-1$. In Equation (4), linear dispersion results from the linear terms in V_n and are proportional to ω_0 while nonlinearities are described by the quadratic terms. The standard nonlinearity is described by terms proportional to α while terms proportional to γ account for the nonlinear diffusion as we will see below and would represent the nonlinear elasticity in mechanical systems [9, 31, 32]. In Equation (4), the presence of the first derivative with respect to time in the term proportional to γ, instead of the second derivative [23], is very important in the formation of pulse signal voltages with compact support. Note that, in the absence of the nonlinear diffusion term, that is, $\gamma = 0$, the network can support both KdV pulse solitons, bright and dark solitary waves of the nonlinear Schrödinger equation [2]. Therefore, γ may be viewed as a parameter that controls the strength of the nonlinear diffusion in the network.

3. NONLINEAR DIFFUSIVE BURGERS' EQUATION

Equation (4) constitutes a set of N differential equations which, in general, cannot be solved exactly. However, in certain parameter regimes, the system allows signal voltage with long wavelength. In this regime (the continuum limit), $V_n(t)$ varies slowly from one cell to another so that the discrete expressions of Equation (4) can be approximated by a third-order Taylor expansion about $V_n(t)$, that is: (i) $2V_n - V_{n-1} - V_{n+1} = -h^2(\partial^2 V/\partial x^2) + O(h^5)$, (ii) $V_{n-1} - V_{n+1} = -2h(\partial V/\partial x) - (h^3/3)(\partial^3 V/\partial x^3) + O(h^5)$, and finally (iii) $(V_n - V_{n+1})^2 - (V_{n-1} - V_n)^2 = (2V_n - V_{n-1} - V_{n+1})(V_{n-1} - V_{n+1}) = 2h^3(\partial V/\partial x)(\partial^2 V/\partial x^2) + O(h^5)$, with $x = nh$ and where h is the lattice spacing. Hence, the exact Equation (4) can be replaced by a continuum representation:

$$\frac{\partial^2 V}{\partial t^2} - \omega_0^2 \frac{\partial^2 V}{\partial x^2} - \alpha \frac{\partial^2 V^2}{\partial t^2} + 2\gamma \frac{\partial}{\partial t}\left(\frac{\partial V}{\partial x}\frac{\partial^2 V}{\partial x^2}\right) = 0, \tag{6}$$

where, without loss of generality, the lattice spacing h is taken equal to 1 so that the space variable x is given in units of cells, which is a more convenient unit for the NLTL.

To solve this equation, we first show that it can be transformed into a nonlinear extension of the Burgers' equation. However, let us mention that, by applying the well-known Garner-Morikawa transformation [2] to the discrete Equation (4), that is, taking $\tau = \epsilon^{3/2}t$, $X = \epsilon^{1/2}(n - \omega_0 t)$ and $V_n = \epsilon\phi(X, \tau)$, the standard nonlinear KdV equation is retrieved and consequently, we cannot appreciate the key-role of the NLR in the network. This means that, the above approximation is not adapted for the derivation of the nonlinear

evolution equation which takes into account NLR effects on the signal voltage in the network. This result is understandable since this transformation rather guarantees the balance between the nonlinearity and the linear dispersion in the series expansion of the wave amplitude. In order to take into account the effects of this nonlinear component in the final approximate equation, we use the following form of the reductive perturbation method which eliminates linear dispersion and guarantees the balance between higher and diffusive nonlinearities:

$$X = \epsilon^0(x - v_p t), \quad \tau = \epsilon^1 t, \quad V = \epsilon\phi(X, \tau), \tag{7}$$

where ϵ is a small parameter measuring the weakness of the amplitude of the signal voltage, and v_p is a constant to be determined. The power of ϵ in X is chosen so that even fast variations of the signal voltage with respect to X (and which characterizes compact structures) are kept in the resulting equation. Substituting Equation (7) into Equation (6) and arranging them in a power series of ϵ, we have a sequence of equations. First, at the leading order of ϵ, i.e., ϵ^1, we have:

$$v_p^2 \frac{\partial^2 \phi}{\partial X^2} - \omega_0^2 \frac{\partial^2 \phi}{\partial X^2} = 0, \tag{8}$$

leading to the following expression for v_p: $v_p = \omega_0$. At the next order, ϵ^2, it follows that:

$$2\frac{\partial}{\partial X}\left(\frac{\partial \phi}{\partial \tau}\right) + (\alpha v_p)\frac{\partial^2 \phi^2}{\partial X^2} + 2\gamma \frac{\partial}{\partial X}\left(\frac{\partial \phi}{\partial X}\frac{\partial^2 \phi}{\partial X^2}\right) = 0. \tag{9}$$

Integrating once this equation with respect to X, with the assumption that $\phi(X, \tau)$ and all its derivatives converge to zero sufficiently rapidly as $X \to \pm\infty$, the following equation is obtained:

$$\begin{aligned} \frac{\partial \phi}{\partial \tau} + (\alpha\omega_0/2)\frac{\partial \phi^2}{\partial X} &= \frac{\partial}{\partial X}\left[D\left(\frac{\partial \phi}{\partial X}\right)\left(\frac{\partial \phi}{\partial X}\right)\right], \\ D\left(\frac{\partial \phi}{\partial X}\right) &= -\frac{\gamma}{2}\left(\frac{\partial \phi}{\partial X}\right), \end{aligned} \tag{10}$$

where $v_p = \omega_0$. This equation appears as a particular case of the one-dimensional $K^*(1,1)$ Cooper-Shepard-Sodano equation as written in Rus and Villatoro [33]. Up to now, its physical interpretation is not yet clear. However, based on equations describing transport properties of physical systems, namely transport and diffusion equations, it can be viewed as a nonlinear convective-diffusive equation where terms proportional to α and γ may describe nonlinear convection and diffusion, respectively. When $\gamma = 0$, Equation (10) reduces to the well-known inviscid Burgers' equation which is a prototype of equations describing shock waves, and has originally been introduced

as a one-dimensional model of turbulence [34]. The case $\gamma \neq 0$ and $D(\partial\phi/\partial X) = \text{const}$ is also known as the Burgers' equation describing many physical phenomena, namely the momentum variation of the viscous fluid, and supports solutions which converge strongly to a weak solution of the inviscid Burgers' equation since the diffusion term simply redistributes energy by dissipation and cannot maintain stability. However, when the diffusivity D is a spatially varying function, as it is the case of Equation (10), the diffusion process is nonlinear and the energy is redistributed via nonlinear interaction and consequently, can provide a stable propagation of a well-defined wave-packet. Accordingly, Equation (10) belongs to a family of *Burgers' equations with nonlinear diffusion* or *nonlinear diffusive Burgers' (NDB) equations*.

Although this NDB Equation (10) is quite different from the well-known Nonlinear Extended KdV (NEKdV) equation introduced by Rosenau and coworkers [1, 35–37], that is, the $K(2,2)$ equation and its extensions, it bears some similar symmetry properties and conserved quantities. For example, as the $K(2,2)$ and $Kq(2,w)$ equations, Equation (10) is invariant under the transformation

$$\phi \to \eta\phi, \quad t \to t/\eta, \quad \eta = \text{const}, \tag{11}$$

and possesses a conservation quantity

$$I_1 = \int \phi dX. \tag{12}$$

This invariance implies that the width of the localized solution of (10) is fixed and independent of the speed. This means that, there is a detailed balance between nonlinear "convection" (term proportional to α) and nonlinear diffusion. Similarly, the invariance of Equation (10) under the transformation (11) with $\eta = -1$ also permits a localized wave with negative amplitude propagating in the opposite direction. To find travelling waves with a constant speed v_c, we define $s = X - v_c\tau$ and integrate once to obtain

$$\left(\frac{d\phi}{ds}\right)^2 = 2\frac{v_c}{\gamma}\phi - \frac{\alpha\omega_0}{\gamma}\phi^2 + C_1, \tag{13}$$

where C_1 is the constant of integration. Various solutions of Equation (13) can be obtained depending on the value of the constant C_1. In this paper we focus our attention on the localized structure. Setting C_1 to zero, it is worth noting that Equation (13) is very similar to the equation obtained for the Rosenau-Hyman case [1]:

$$\left(\frac{d\phi}{d\tau}\right)^2 = \frac{2v}{n(n+1)}\phi^{3-n} - \frac{2}{n(n+m)}\phi^{m-n+2}. \tag{14}$$

Thus, we see that with $m = n = 2$, the equation for finding the solution is identical in form, with only differing coefficients. Therefore we expect to find similar solutions to Equation (13). Considering the variable change, $\phi = 2(v_c/\alpha\omega_0)u^2$, Equation (13) takes the simple form:

$$\left(\frac{du}{ds}\right)^2 = \frac{\alpha\omega_0}{4\gamma}\left(1-u^2\right), \tag{15}$$

which admits a solitary wave with a compact support

$$u(s) = \begin{cases} \cos(k_c s) & |s| \le \pi/2k_c \\ 0, & |s| > \pi/2k_c, \end{cases} \tag{16}$$

with width parameter

$$k_c = \sqrt{\frac{\alpha\omega_0}{4\gamma}}, \tag{17}$$

provided that $\alpha\gamma > 0$. By using original variables, the solitary wave's solution of the NDB Equation (10) is then given by:

$$\phi(X,\tau) = \begin{cases} A_0\cos^2[k_c\,(x - v_c\tau)], & |\,(x - v_c\tau)\,| \le \pi/2k_c \\ 0, & |\,(x - v_c\tau)\,| > \pi/2k_c, \end{cases} \tag{18}$$

with the speed proportional to the amplitude A_0:

$$v_c = \frac{\alpha\omega_0}{2}A_0. \tag{19}$$

This dependence of the wave's speed on its amplitude and the non-dependence of the width to the speed are in full agreement with the scaling of solutions described by Equation (10). This result is also in accordance with the original result by Rosenau and Hyman [1] and those obtained by Cooper et al. [38], and Rus and Villatoro [33]. From Equations (17) and (19), it appears that the pulse's characteristic parameters are functions of the nonlinear coefficient of the system, that is α and γ. In addition, the fact that the width parameter is inversely proportional to γ clearly shows that the existence of the compact solution (18) is closely connected to the existence of the nonlinear diffusion in the network resulting from the NLR. The dependence of the diffusivity D on the gradient $\partial\phi/\partial X$ reduces smoothing at edges of the wave and is then responsible for the formation a compact wave. Similar results have also been obtained by Comte and Marquié [22] in the reaction-diffusion equation modeling the propagation of fluxons (kink with compact support) in a NLTL where the compactification of kinks originates from the nonlinear diffusion process.

Before ending this section, it is useful to make a comparison between parameters of the compacton of the well-known $K(2,2)$ equation and those of the compact solitary wave described by the

nonlinear diffusive Burgers' Equation (10). Let us mention that, we have no intention to compare two quite different physical phenomena but to compare the width and speed of the pulse, resulting from each of these phenomena, which are important characteristics for signal processing. For this purpose, it is convenient to rewrite Equation (10) in the following form:

$$\frac{\partial \phi}{\partial \tau} + (\alpha\omega_0/2)\frac{\partial \phi^2}{\partial X} + \sigma\frac{\partial^3 \phi^2}{\partial X^3} + \nu\phi\frac{\partial^3 \phi}{\partial X^3} = 0, \tag{20}$$

where $\sigma = \gamma/6$ and $\nu = -\gamma/3$. Equation (20) with arbitrary coefficients is an extension of the $K(2,2)$ equation and reduces to the $K(2,2)$ equation when $\nu = 0$. It admits the same $\cos^2$-shape as a compact solution, that is, $\phi = A_0\cos^2[k(x - vt)]$ with the corresponding pulse parameters: $k^2 = \alpha\omega_0/4(\nu+8\sigma)$ for the width and $v = 12\sigma A_0 k^2$ for the speed. Taking $\nu = 0$, these parameters reduce to the $K(2,2)$ compacton parameters, that is, $k^2 \equiv k_{RH}^2 = \alpha\omega_0/(32\sigma)$ and $v \equiv v_{RH} = 3\alpha\omega_0 A_0/8$. If $\nu < 0$ the pulse parameter k is then enhanced leading to the increase of the speed v while the resulting pulse width which is inversely proportional to k is lowered. Accordingly, the compact pulse of the NDB Equation (20) for which $\nu = -\gamma/3 < 0$ is more narrow and moves faster than the Rosenau-Hyman $K(2,2)$ compactons.

4. COMPACTLY-SUPPORTED SIGNAL VOLTAGE

4.1. Approximated Expression

In this subsection, we derive the approximate analytical expression of the signal voltage, solution of the circuit Equation (4). By combining Equations (7), (18) and (19), the analytical expressions are obtained as follows:

$$V_n(t) = \begin{cases} V_m\cos^2[k_c\,(n - v_g t)], & |\,(n - v_g t)\,| \le \pi/2k_c \\ 0, & |\,(n - v_g t)\,| > \pi/2k_c. \end{cases} \tag{21}$$

with

$$v_g = \omega_0\left(1 + \alpha\frac{V_m}{2}\right). \tag{22}$$

This expression describes the approximated analytical expression of the compactly supported signal voltage with the amplitude $V_m = \epsilon A_0$, valid only for large width, that is, for $k_c \ll 1$, where k_c is well defined by Equation (17). However, in contrast to this width parameter, the velocity of the compact signal is now defined by Equation (22) with a new relationship between compact pulse's amplitude and width. This

modification of the speed-amplitude relationship of the compact signal may have some consequences on the behavior of compact electrical voltage pulses on the network. For example, since α and V_m are both the small parameters, the speed of the compact electrical voltage pulses will be almost constant in practice for different amplitudes, in contrast to the pulse solution (16) where its speed is proportional to the amplitude.

4.2. Exact Solution

We derive here an exact solution, of the set of differential Equation (4), valid not only for pulse signal voltages with a large width but also for pulse signals with small width. For this purpose, on the basis of the result of the preceding section, we use expression (21) as a trial function where in this case k_c and v_g are the unknown constants to be determined. Here, our goal consists in demonstrating the accuracy of the approximation performed in the preceding section to obtain an analytical solution in the continuum limit. By inserting the above expression in the set of discrete differential Equation (4), after evaluating the terms $V_{n\pm1}(t)$, $V_n(t)^2$ and $V_{n\pm1}(t)^2$, the system of equations verified by the wave parameters are obtained as follows:

$$\omega_0^2[1-\cos(2k_c)] - 2k_c^2 v_g^2(1-\alpha V_m) = 0, \tag{23}$$

and

$$\alpha k_c v_g - \gamma \sin(2k_c)\,[1-\cos(2k_c)] = 0. \tag{24}$$

Before solving these two coupled equations, let us mention that the constant k_c is the width parameter of the wave while the full width is strictly limited to $L_c = \pi/k_c$. However, since the formation of this compact structure requires participation of at least three cells, the minimum value of the width is then $L_c = 2$ leading to the maximum value of the width parameter $k_{\max} = \pi/2$. For this particular case, that is $k_c = k_{\max}$, the wave centered at site n_0 covers the sites $n_0 - 1$, n_0 and $n_0 + 1$ where $n_0 \pm 1$ are edges of the compact wave, and admits as velocity $v_s = 0$ provided that $\omega_0 = 0$. This means that the existence of this static compact wave is possible only if the linear dispersion in the network is absent, that is, when the linear inductor L is suppressed in the NLTL illustrated in Figure 1. Similar results have also been obtained by Comte and Marquié [22] where they determined the static compact-like kink in an RC electrical reaction diffusion chain.

When $\omega_0 \neq 0$, Equations (23) and (24) admit the following solution:

$$v_g = \frac{\omega_0}{\sqrt{1-\alpha V_m}} \frac{\sin(k_c)}{k_c}, \tag{25}$$

and

$$2\sin(k_c)\sin(2k_c) = \frac{\alpha\omega_0}{\gamma\sqrt{1-\alpha V_m}}. \tag{26}$$

with $0 < k_c < \pi/2$. Expression (21) with speed and width given by Equations (25) and (26), respectively, describes discrete solitary waves with the compact support solution of circuit Equation (4). Thus, the compact solitary wave has a definite velocity when its amplitude and width are given. However, in contrast to compacton properties where the width is independent of the amplitude, from Equations (25) and (26), it appears first that, the width of the discrete compact solitary wave is amplitude dependent due to the intrinsic discrete character of the network. This dependence may become negligible if the amplitude of the signal voltage and the strength of the standard nonlinearity α are both small compared to 1. Next, in the limit of small width parameter ($k_c \to 0$) and signal amplitude V_m, these compact solitary wave parameters (25)–(26) reduce to Equations (17) and (22) which are results previously obtained in the continuum limit. Thus, three remarks can be made:

- Firstly, the NDB Equation (10) may adequately describe the dynamics of a compact pulse with large width in the network only for small amplitude voltage and in the mobile reference frame.
- Next, the discrete nature of the system associated to the presence of a linear dispersion may modify the relationship between the compact wave amplitude, speed and width.
- Finally, when $\gamma = 0$, the set of differential Equation (4) admits, in the continuum limit, the well-known KdV sech^2-type pulse soliton [2]. Accordingly, Equation (4) appears as a discrete nonlinear equation for the NLTL exhibiting a compact-version of the KdV pulse soliton. However, as we shall see in the numerical simulations of the line, this discrete solution of the compact pulse could not propagate stably until its width is large enough to annihilate the discreteness effects of the network.

5. DISSIPATIVE EFFECTS OF THE NETWORK

In real physical systems, dissipative effects coexist together with nonlinear and dispersive effects and may play some role in a wave generation and its propagation. Among many effects of dissipation on the wave motion, we focus our attention on the decrease of the amplitude of the wave. In the network under consideration, this dissipation results from electrical elements such as the linear inductor L. It may also be introduced by the use of the real diode to describe

the NLR instead of the quadratic one. These dissipation effects may be adequately described by the first term of the NLR, that is $a\delta V_n$ with $a > 0$. From Kirchhoff's laws, it is then straightforward to observe that the propagation of the signal voltage in the network is governed by the following system of equations:

$$\begin{aligned} &\frac{d^2V_n}{dt^2} + \left(\omega_0^2 + g\frac{d}{dt}\right)(2V_n - V_{n-1} - V_{n+1}) \\ &= \alpha\frac{d^2V_n^2}{dt^2} - \gamma\frac{d}{dt}\left[(V_n - V_{n+1})^2 - (V_{n-1} - V_n)^2\right] \end{aligned} \tag{27}$$

for $n = 1, 2, \ldots, N-1$ and where $g = a/C_0$. Let us mention that, since the dissipation term is usually a small perturbation, its contribution is often neglected. Hence, we assume that this term is weak and is of the order of ϵ^2, where ϵ is a small parameter, that is, $g \equiv \epsilon^2\lambda$. Under this condition, using the standard continuum approximation at one order higher than the nonlinear extended KdV-type Equation (10), associated with the reductive perturbation method (7), Equation (27) leads to the following equation for ϕ:

$$\frac{\partial\phi}{\partial\tau} + (\alpha\omega_0/2)\frac{\partial\phi^2}{\partial X} + \gamma\frac{\partial\phi}{\partial X}\frac{\partial^2\phi}{\partial X^2} = \epsilon R[\phi], \tag{28}$$

with

$$R[\phi] = \frac{\lambda}{2}\frac{\partial^2\phi}{\partial X^2}, \tag{29}$$

where $R[\phi]$ can be viewed as the perturbation on the compact pulse motion. In order to derive the quantitative effects of this perturbation on the pulse parameters, we use an approach based on the multiple time scale expansion [39]. Although this approach has proved to be particularly convenient for studying the time dependent perturbations on standard soliton motion, our analysis shows that it can be also satisfactorily applied to nonlinear evolution equations that admit solitons with compact shape.

Firstly, the independent variable is transformed into several variables by $\tau_m = \epsilon^m\tau$, $m = 0, 1, 2, \ldots$ where each τ_m is an order of ϵ smaller than the previous time. At the same time, ϕ and $R[\phi]$ are expanded in an asymptotic series:

$$\phi = \phi_0 + \epsilon\phi_1 + \ldots \quad R[\phi] = R^0[\phi_0] + \epsilon R^1[\phi_0, \phi_1] + \ldots \tag{30}$$

Next, substituting Equation (30) into Equations (28) and (29), and equating the coefficients of each power of ϵ, we obtain the following equations: At order ϵ^0:

$$\frac{\partial\phi_0}{\partial\tau_0} + (\alpha\omega_0/2)\frac{\partial\phi_0^2}{\partial X} + \gamma\frac{\partial\phi_0}{\partial X}\frac{\partial^2\phi_0}{\partial X^2} = 0, \tag{31}$$

and at order ϵ^1:

$$\widehat{L}(\phi_1) = R^{(0)}[\phi_0] - \frac{\partial \phi_0}{\partial \tau_1}, \tag{32}$$

where $\widehat{L}$ is a linear differential operator defined by

$$\widehat{L} = \frac{\partial}{\partial \tau_0} + \alpha\omega_0 \left(\phi_0 \frac{\partial}{\partial X} + \frac{\partial \phi_0}{\partial X} \right) + \gamma \left(\frac{\partial \phi_0}{\partial X} \frac{\partial^2}{\partial X^2} + \frac{\partial^2 \phi_0}{\partial X^2} \frac{\partial}{\partial X} \right). \tag{33}$$

and the adjoint operator of $\widehat{L}$ is given by:

$$\widehat{L^*}(\rho) \equiv \left(\frac{\partial}{\partial \tau_0} + \alpha\omega_0\phi_0 \frac{\partial}{\partial X} + \gamma \frac{\partial \phi_0}{\partial X} \frac{\partial^2}{\partial X^2} \right) \rho = 0, \tag{34}$$

where $\rho(X, \tau_0, \tau_1) = \int_{-\infty}^{X} \varphi(\zeta) d\zeta$ and where φ is one of the solutions of $\widehat{L}$. Multiplying (32) by ρ and integrating with respect to X, we obtain after having taken into account Equation (34) and the boundary conditions $\lim_{X \longrightarrow \pm\infty} \phi_\beta = 0$ and $\lim_{X \longrightarrow \pm\infty} \partial^\mu \phi_\beta / \partial X^\mu = 0$ with $\beta = 0$, 1 and $\mu = 1$, 2:

$$\frac{\partial}{\partial \tau_0} \int_{-\pi/2k_c}^{+\pi/2k_c} \rho\phi_1 d\eta = \int_{-\pi/2k_c}^{+\pi/2k_c} \rho \left\{ R^{(0)}[\phi_0] - \frac{\partial \phi_0}{\partial \tau_1} \right\} d\eta, \tag{35}$$

which is the evolution equation for ϕ_1. Since ρ depends on X and τ_0 only through the combination $X - v_c\tau_0$, the τ_0 dependence of the integrand on the right-hand side vanishes by the space integration and consequently, the perturbation ϕ_1 behaves secularly in τ_0. In order to eliminate this secularity, one requires that the integral on the right hand side of Equation (35) must be zero; leading to the non secular conditions:

$$\int_{-\pi/2k_c}^{+\pi/2k_c} \rho_i \left\{ R^{(0)}[\phi_0] - \frac{\partial \phi_0}{\partial \tau_1} \right\} d\eta, \quad i = 1, 2, \tag{36}$$

where

$$\rho_1(X, \tau_0, \tau_1) = \int_{-\infty}^{X} \frac{\partial \phi_0}{\partial \xi} d\zeta, \quad \rho_2(X, \tau_0, \tau_1) = \int_{-\infty}^{X} \frac{\partial \phi_0}{\partial \widetilde{a}} d\zeta. \tag{37}$$

The function ϕ_0 is the solution of the unperturbed Equation (31), that is,

$$\phi_0(\eta) = \begin{cases} \widetilde{a}\cos^2(k_c\eta), & |(\eta)| \leq \pi/2k_c \\ 0, & |(\eta)| > \pi/2k_c. \end{cases} \tag{38}$$

with $\eta = X - \xi$. By combining Equations (36)–(38), the system of two differential equations governing the modulation of compact solitary wave parameters is obtained as follows:

$$\begin{cases} \frac{\partial \widetilde{a}}{\partial \tau_1} + \frac{2}{3}\lambda k_c \widetilde{a} = 0, \\ \frac{1}{3}\frac{\pi}{k_c}\frac{\partial \widetilde{a}}{\partial \tau_1} + \frac{3}{8}\widetilde{a}\frac{\partial \xi}{\partial \tau_1} = 0, \end{cases} \tag{39}$$

and which admits the solution:

$$\widetilde{a}(\tau_1) = A_0 \exp\left[-\frac{2}{3}\lambda k_c^2 \tau_1\right], \quad \xi(\tau_1) = \frac{16}{27}\pi\lambda k_c \tau_1 + \xi_0, \qquad (40)$$

where A_0 and $\xi_0 = v_c\tau_0$ are the parameters of the unperturbed compact pulse. Finally, with the above expressions, the compact-like signal voltage which takes into account the dissipation of the network is given by:

$$V_n(t) = \begin{cases} V_m \exp\left[-\frac{2}{3}gk_c^2 t\right] \cos^2\left[k_c\left(n - v_\varsigma t\right)\right], & |\left(n - v_\varsigma t\right)| \leq \pi/2k_c \\ 0, & |\left(n - v_\varsigma t\right)| > \pi/2k_c. \end{cases} \qquad (41)$$

where $v_\varsigma/\omega_0 = (1 + \alpha\frac{V_m}{2}) + \delta v/\omega_0$ is the compact pulse's speed along the network, the parameter $\delta v/\omega_0 = (16/27)\pi g k_c^2/\omega_0$ being the small constant speed shift induced by the dissipation of the network. Similarly, the amplitude decays exponentially with time with the decreasing rate proportional to the square of the pulse width. This result is qualitatively in full agreement with the results previously obtained by Rosenau and Pikovsky [13] and recently by Rus and Villatoro [40] by means of conserved quantities of the $K(2,2)$ equation. However, the fact that the speed of the compact pulse experiences a constant shift is in contrast with their results since, they pointed out that, the perturbation can cause a damping and deceleration or a growth and acceleration, of compact pulse solitary waves.

6. NUMERICAL RESULTS AND SIMULATIONS

In this section, we present the details and the results of numerical integrations performed both on the exact discrete equations governing wave propagation along the NLTL (4) as well as on the NDB-type Equation (10) describing the dynamics, in the moving frame of reference, of small-amplitude waves in the network. The numerical values for each electrical component of the NLTL are listed in Table 1: The nonlinear capacitance which, as an example, is taken as an accumulation-mode: Metal-Oxide Semiconductor Varactor (MOSVAR) [18] with a dc-bias voltage $V_b = 1.5\,\mathrm{V}$. The coefficient b characterizing the NLR is given in Table 1.

6.1. Nonlinear Diffusive Burgers' Equation: Pulse Compactons

To perform numerical integrations of the NDB Equation (10), the fourth-order Adams-Bashforth-Moulton predictor corrector method in time and the finite difference method in space are used. Finite

Table 1. Parameters of numerical integrations of the dimensionless NDB-type Equation (42) plotted in Figure 4, and those of the discrete circuit's Equation (4) of the NLTL plotted in Figures 5, 6 and 7.

Equations	Parameters	Symbols	Numerical values
NDB-type Equation (42)	Spatial grid point	N	1024
	Length of interval	L	400
	Integration time step	ΔT	0.0011
	Pulse Amplitude	A_0	0.04
	Pulse Width	k_c	0.5
Circuit Equation (4)	Dissipation coefficient	a	$3.8681 \times 10^{-7}\,\Omega^{-1}$
	Diffusive nonlinearity coefficient	b	$7.4809 \times 10^{-6}\,\mathrm{AV}^{-2}$
	Inductance	L	0.8 H
	Capacitance	C_0	1 pF
	Standard nonlinearity coefficient	α	$0.25\,\mathrm{V}^{-1}$
	Integration time step	h	0.001
	Pulse signal width	L_c	32.5 cells
	Pulse signal amplitude	V_m	0.1 V

difference method is implemented in the computer by means of the gradient function of the MATLAB toolbox. To take care with the scale of the studied phenomena, Equation (10) is rewritten in the following dimensionless form:

$$\frac{\partial \phi}{\partial T} + \frac{\partial}{\partial z}\left(\phi^2\right) + \frac{\partial}{\partial z}\left[\left(\frac{\partial \phi}{\partial z}\right)^2\right] = 0, \tag{42}$$

where $T = (\alpha\omega_0/2)\sqrt{\alpha\omega_0/\gamma}\tau$ and $z = \sqrt{\alpha\omega_0/\gamma}X$ are the dimensionless variables and which admits the following compact solitary wave solution:

$$\phi = A_0 \cos^2[(z - z_0 - v_e T)/2], \quad v_e = A_0. \tag{43}$$

For this solution, the exact value of the conserved quantity $I_1 = \pi A_0$. The problem (42) is solved on the interval $-L/2 \leq z \leq L/2$ with L and N are listed in Table 1 and initial conditions given by Equation (43). As is well known, the nonlinear KdV and its extension are numerically difficult to solve due to the presence of higher order dispersion terms. The problem becomes even more difficult when the nonlinear dispersion or nonlinear diffusion-like terms are present. To overcome this difficulty, the integration time step ΔT is chosen so that $\Delta T = \chi(\Delta z)^3$ where χ is a constant. This constraint improves the

stability of the numerical scheme. In the simulation, the coefficient $\chi = 0.0185$ is also chosen so that aliasing errors which could dominate the numerical integration of the NDB equation are minimized. In addition, in order to gain insight into the accuracy of the numerical method and because of the lack of the quadractic conserved quantity for this system, the conserved quantity I_1 is calculated and compared with the exact value. In our simulations, the integration time step and the length Δz are chosen to preserve this conserved quantity to an accuracy better than 10^4 over a complete run. Figure 2 shows the result of this simulation where the compact pulse initially located at $z_0 = -200$ experiences a uniform propagation without a noticeable change of its form and with velocity $v_e = 0.05$ which is in agreement with the analytical prediction. This numerical experiment confirms the

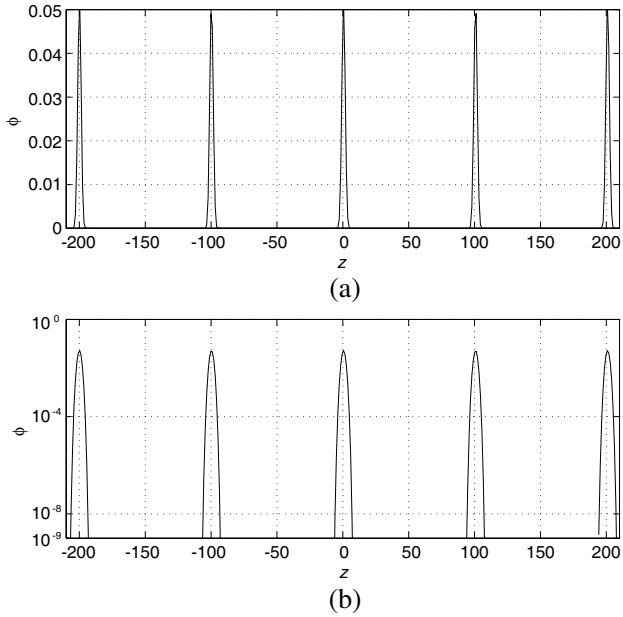

Figure 2. Propagation of compact pulse solitary wave starting with the center at $z_0 = -200$, with amplitude $A_0 = 0.05$ and width parameter $k_c = 0.5$, simulated on the nonlinear diffusive Burgers Equation (42). The top panel (a) shows the waveforms at given dimensionless times of propagation: T_0, $2T_0$, $3T_0$ and $4T_0$, respectively, with $T_0 = 2000$, while the bottom panel (b) shows the same profile in logarithm scale. This behavior confirms the uniform propagation of the compact solitary wave with reduced velocity $v_e = A_0 = 0.05$, as predicted by the analytical result.

fact that expression (43) is a strong solution of the NDB Equation (10).

In order to check the properties of this compact pulse solitary wave, the simulations are performed with two and three compact pulses with different amplitudes and located at different positions, each of them described by Equation (43). Figure 3 firstly shows the collision between two compact pulses with different amplitude and next, the propagation of three pulses in the same direction leading finally to their collision. Since the taller one moves faster than the shorter one, it catches up and collides with the shorter one and then moves away from it as time increases. As outlined by Rosenau and Hyman [1], these numerical simulations show also that the point where compactons collide is marked by the creation of very small compact wave (amplitude $\sim 10^{-3}$) and which very slowly evolves into compacton-anticompacton pairs. Some other experiments are done, notably the head-on collision between a compact pulse and an anticompact pulse and the results indicate that the compact pulse survives through collisions.

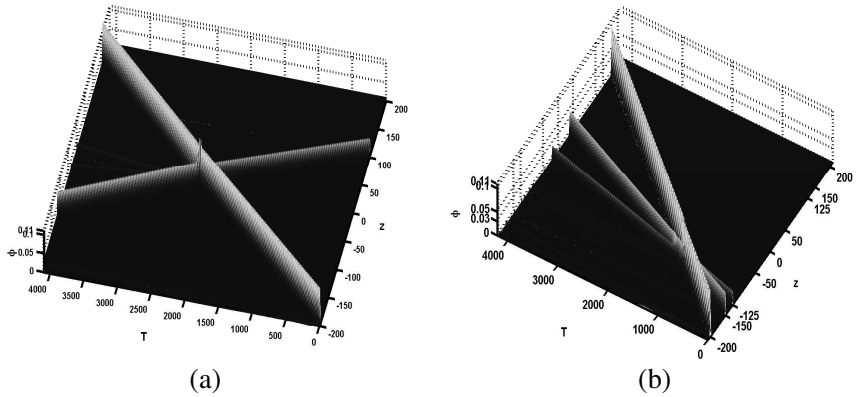

Figure 3. Propagation and head-on collision between (a) two and (b) three compact solitary waves. Initially theses wave are localized at positions $z = -200$ and $z = 100$ for the first case and for the second case at the positions $z = -200$, -150 and -125. In this later case, pulses have different amplitudes $A_0 = 0.1$, 0.05 and 0.03 propagating in the same direction. The waves maintain their shape after collision.

Now, taking as initial conditions for the numerical simulations of the NDB Equation (10), a compact wave-packet with a width two times larger than that of the exact compact pulse solitary wave described by Equation (17), as presented in Figure 4, the solution decomposes into many compact pulses with the taller one far from the shorter one.

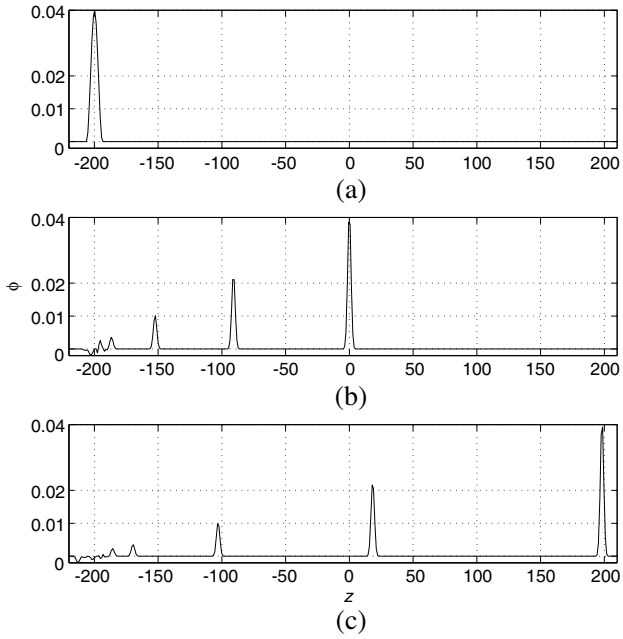

Figure 4. Propagation of a compact wave. (a) Initially the width of the wave-packet is two times larger than that of the exact compact wave (43), i.e., $k = k_c/2 = 0.25$; subplots (b) and (c) show the decomposition of this wave-packet at given dimensionless times of propagation: $T_0 = 4875$ and $2T_0$, respectively.

This result is in full agreement with the result previously obtained by Rosenau and Hyman [1]. However, it is early to make a strong conclusion on the possibility of this compact pulse (18), solution of the NDB-type Equation (10), exhibiting all the relevant properties of the $K(2,2)$ compactons.

6.2. Electrical Pulse Compacton

To check whether the NDB Equation (10), which is an approximation of the exact discrete equation, is a fairly accurate description of signal dynamics along the network, we perform numerical integrations of the exact discrete Equation (4) with different initial conditions. The fourth order Runge-Kutta scheme in time is used with normalized integration time step $h = \omega_0 \Delta t = 0.001$ corresponding to the sample period $T_s = 8.94\,\text{ns}$. In addition, in order to avoid signal reflection at the end of the line and also to run experiments with sufficiently large time,

the number of cells of the network is taken between 10^3 and 11×10^3 and varies from one experiment to another. To observe the propagation of signal voltages we use, as initial condition, the following compactly-supported signal voltage of amplitude V_m:

$$V_n(t) = V_m \cos^2[k_c\,(n - v_g t)], \quad \text{for} \quad |\,(n - v_g t)\,| \leq \pi/2k_c \qquad (44)$$

and $V_n(t) = 0$ otherwise, predicted by Equation (21). The corresponding pulse width is $L_c = \pi/k_c$, corresponding to the temporal compact wave width $\tau_s = L_c/v_s = 28.7\,\mu$s. As shown in Figure 5 the initial electrical pulse propagates with the same amplitude, without distortion of shape, and with constant velocity 1132 cells/ms which

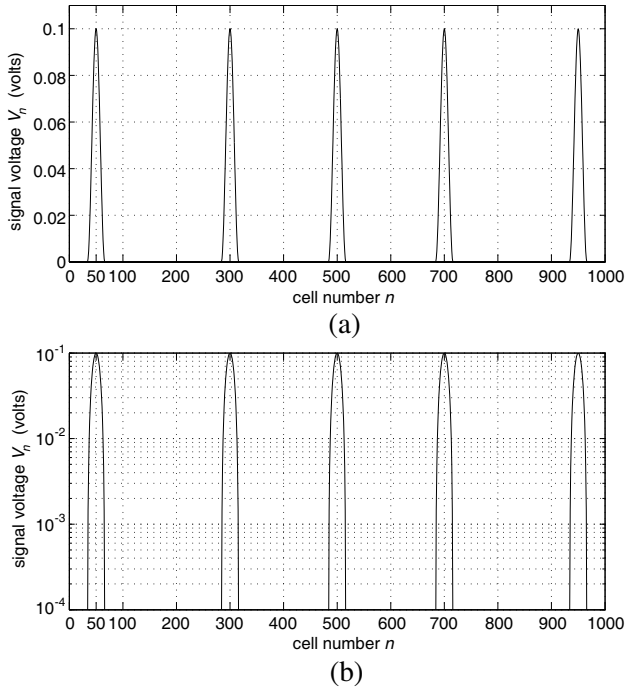

Figure 5. Stable and uniform propagation of the compactly-supported signal voltage along the lumped nonlinear electrical transmission line. The network parameters and those of the initial compact pulse signal are given in Table 1. The top panel (a) shows the waveforms at given dimensionless times of propagation: $\omega_0 t = 250$, 450, 650 and 900, respectively, while the bottom panel (b) shows this profile in logarithm scale. This behavior confirms the uniform propagation of a compact solitary wave with reduced velocity $v_s/\omega_0 = 1.012$, that is, $v_s = 1132$ cells/ms, as predicted by the analytical result.

corresponds to the analytical predicted value. Because of the smallness of the width parameter k_c, this compact wave may be viewed as the continuum solitary wave with compact support propagating along the continuum medium, the NLTL. However, when the compact wave width L_c is close to 1, one observes that the corresponding compact wave disintegrates into oscillatory waves during its propagation along the network. This means that discrete NLTL may not exhibit stable traveling compact waves. This result is also in agrement with the result previously obtained by Kevrekidis et al. [8] when analyzing traveling compactons in discrete models using the quantization condition.

To check another property devoted to compactons, we have also

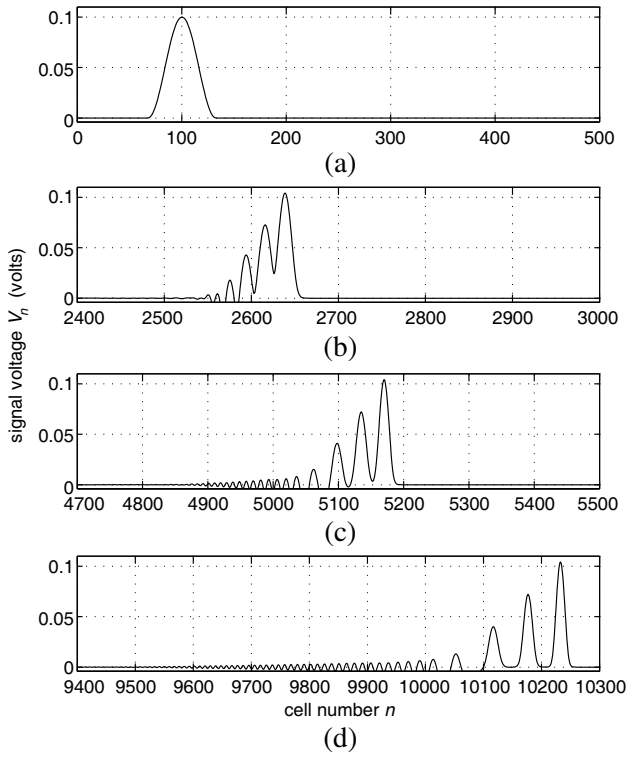

Figure 6. Propagation along the non dissipative NLTL of the compact electrical pulse signal. (a) Initially the width of this signal voltage centered at cell 100 is two times larger than that of the exact compact signal exhibited by this network (17), i.e., $L = 2L_c$; subplots (b), (c) and (d) show its decomposition at given dimensionless times of propagation: $\omega_0 t_0 = 2575$, $2\omega_0 t_0$ and $4\omega_0 t_0$, respectively.

performed numerical integrations of the exact Equation (4) with initial conditions given by (44), but with pulse width two times larger than the exact compact pulse signal voltage, that is, $L = 65$ cells. As presented in Figure 6, the disintegration of this wide compact pulse signal voltage into a set of compact pulse signals of different amplitudes moving with the corresponding velocity is observed after long time dynamics in the network. However, in contrast to the behaviour of pulse compacton of the NDB equation, the number of compactons resulting from the disintegration is very high. Similar results have been obtained by Rosenau and Pikovsky [13] in the discrete nonlinear dispersive models without linear dispersion, and with an additional feature, not observed here; the birth of kovatons which are a compact formation of glued together kink-antikink pairs that may assume an arbitrary width. Accordingly, this great number of compact pulses may result from the discrete nature of the system.

In order to take into account dissipation effects on the propagation of compact pulse signal voltages given by (44), we have also integrated numerically the discrete Equation (4) with a (see Table 1). The stable propagation of the initial compact signal is observed, but with the decrease of its amplitude, as illustrated in Figure 7(a). When the initial pulse is considered with width larger than the exact compact pulse (17), the numerical experiment shows that this arbitrary data propagates without any disintegration as in the non-dissipation model. However, the amplitude of the pulse reduces less compared to that of the exact compact-pulse signal voltage with the same initial amplitude [see Figure 7(b)]. This means that, the decreasing rate of the amplitude, due to dissipation effects, is a decreasing function of the pulse width. This result is in accordance with the analytical predictions of section 5 [see Equation (41)]. Thus, dissipation effects on the amplitude of the compact pulse signal voltage may be minimized by the widening of the compact pulse.

Beside these results, Figure 7 shows also that the compact pulse signal voltage, under dissipation, widens as the amplitude decreases, in contradiction to the analytical results of Section 5 where it is shown that the amplitude of the compacton decreases but without changing its width. In addition, this wave packet maintains their form (no disintegration) in the considered time of experimentation. Since the rate of amplitude damping in both NDB compactons and the KdV solitons are similar, one can intuitively interpret this behavior as a transformation of a NDB compacton into a KdV soliton during its propagation. However, on the basis of the numerical experiments performed on the non-dissipative NLTL, [see Figures 5 and 6], it is clear that the undamped compact signal voltage keeps its form unchanged

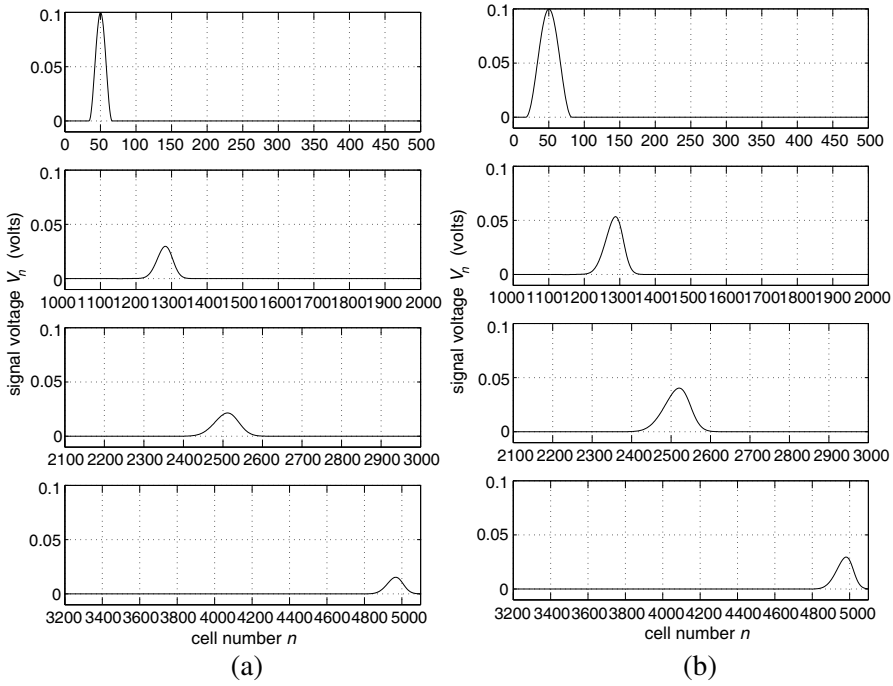

Figure 7. Decrease of the amplitude of the compact signal voltage due to the dissipation in the network. (a) Exact compactly supported signal voltage described by Equation (21). (b) Arbitrary compact signal voltage with width two times larger than that of the exact compact signal voltage, i.e., $L = 2L_c$. The amplitude of this arbitrary compact signal decreases less compared to that of the exact compact pulse. The initial compact signal is located at cell $n_0 = 50$ while the subplots (2), (3) and (4) show the waveform at dimensionless time $\omega_0 t_0 = 1215$, $2\omega_0 t_0$ and $4\omega_0 t_0$, respectively.

and bears some compacton properties, observed in discrete nonlinear dispersive models without linear dispersion, such as the disintegration of compact pulse into a set of compact pulse with different amplitudes which are not observed in the Toda lattice modelling the dynamics of discrete KdV solitons. In addition, experiments on KdV solitons performed in the NLTL under consideration, not presented here, exhibit an unstable behaviour until the nonlinear resistance parameter γ is taken equal to zero. This means that the presence of the nonlinear diffusive term in the network destabilizes the KdV soliton. Nevertheless, effects of the linear dispersion and dissipation on the

compact structures are still an outstanding problem and deserve to be carefully examined. The work on this issue is now under consideration.

6.3. Implementation and Simulations

The NLTL under consideration has been implemented and simulated by means of the Pspice software using realistic components for circuit simulations. In fact, the following characteristic parameters of the line are considered: the line polarization voltage $V_b = 1.5\,\mathrm{V}$ and $L = 0.8\,\mathrm{H}$ for the inductor. The nonlinear capacitor in the shunt branch is the $BAS32$ diode, a European diode with $C_0 = 1\,\mathrm{pF}$ and associated resistance $R = 0.84\,\Omega$. As for the NLR which is responsible for the compactification of the signal, we consider the $BAY80$'s diode model with $I_s = 10.64\,\mathrm{nA}$. These values of the NLTL components permit a

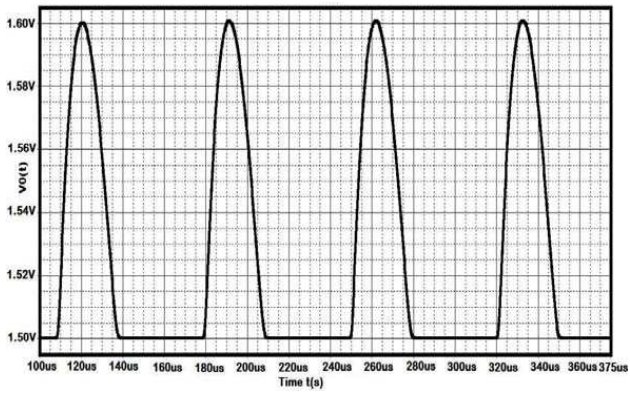

(a)

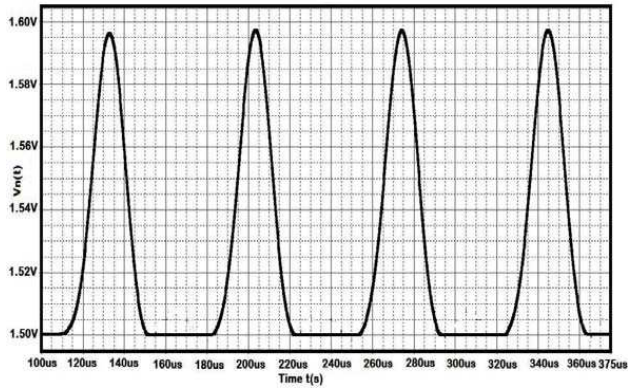

(b)

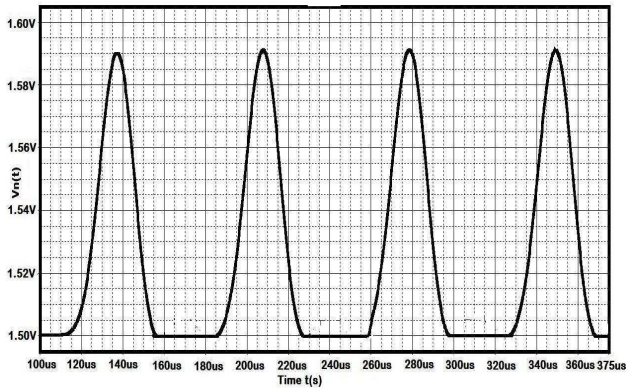

(c)

Figure 8. Results of simulations of the NLTL by means of the PSPICE professional. compact-like pulse signals at three different cells of the NLTL: (a) Input signal, (b) cell 60 and (c) cell 100. The amplitude of the signal at cell 60 is smaller than that of the input signal due to the dissipation effects induced by the losses of the NLTL. The numerical values of the circuit element are given in Section 6. Note that the signal voltage $V_n(t)$ varies from 1.5 V to a maximum value due to the polarization voltage $V_b = 1.5\,\mathrm{V}$ applied to each cell of the line.

pulse signal with compact shape and temporal width $\tau = 29.6\,\mu\mathrm{s}$ which is related to the spatial width L_s through the expression $L_s = v_c\tau$ with $v_c = 1132\,\mathrm{cells/ms}$ the pulse's speed. Figure 8 shows a train of compact pulse signal voltages at given cells of the NLTL. It is obvious that the compact pulse voltages propagate without distortion of shape. However the amplitude decreases due to dissipation effects induced by the losses of the NLTL. This simulation evidences the fact that the NLTL under consideration is a good medium for the propagation of pulse signal voltages with compact shape. Nevertheless it important to mention that for these simulations the input signal voltage must be carefully chosen so that it shape matches the theoretical compact pulse described by Equations (25) and (26) [see [41] for more informations].

7. CONCLUDING REMARKS

In this paper we have introduced and investigated a discrete nonlinear electrical transmission line (NLTL) with nonlinear intersite resistance exhibiting pulse signal voltages with compact shape. More precisely, we have first shown that, shunting the linear inductor in each cell of the

basic LC electrical transmission line by a nonlinear resistance (NLR), the quadratic diode for example, induces a nonlinear diffusion term in the circuit equations. In the continuum limit and by making use of the reductive perturbation method which takes into account fast variations of the signal voltage with respect to space and time, we have derived a partial differential equation belonging to the family of nonlinear diffusive Burgers' (NDB) equations whose properties are similar to those of the well known Rosenau-Hyman $K(2,2)$ equation [1]. This equation appears as a particular case of the one-dimensional $K^*(1,1)$ Cooper-Shepard-Sodano equation as written in Rus and Villatoro [33] and, as expected, exhibits pulse compacton as an exact analytic solution with width independent of the amplitude while the speed is amplitude dependent.

Next, the above study has been completed by the investigation of losses of circuit components on the compacton propagation where we have shown that, the Tanaka's perturbation method [39] can be also satisfactorily applied to the NDB equation which admits a solitary wave with compact shape. However, taking into account the discrete nature of the system associated to a linear dispersion, the speed-amplitude relationship of the compact signal voltage is modified since the signal's speed takes into account the group velocity of all wave-packets propagating in the system. Accordingly, the speed of the compact signal voltage may slightly depend on the amplitude of the wave and then, some compacton properties such as the decomposition of the initial compact data wider than the exact compacton pulse into several independent compactons would be only observed experimentally rather after long time dynamics of the signal.

Finally, these results have been checked by means of numerical simulations both of the NDB equation and of the NLTL, where some additional features have been observed, notably the elastic collision of the compact pulse of the NDB equation which is accompanied by the birth of compact small oscillations from the impact area and which evolve into compact pulses of very small amplitudes as pointed out by Rosenau and Hyman [1], the decomposition of the arbitrary compact wave into several independent compact pulses on the NDB equation as well as on the NLTL. As a matter of fact, the obtained compact wave shares many important properties with the Rosenau and Hyman compactons. However, although our results on dissipation effects show some agreements between numerical and analytical results, these effects as well as those of the linear dispersion on the behavior of compact structures deserve a particular attention. The work on this issue is now under consideration.

Before ending this paper, let us mention that the electrical pulse

signals are primarily utilized for sharp pulse generation, which is of considerable interest in modern electronics. In ultra-fast time-domain metrology, the short duration of a pulse directly translates to a high temporal resolution, and hence, narrow electrical pulses can be used to sample rapidly varying signals or as probe signals for high-precision time-domain reflectometry. In addition, periodic sharp compact pulse trains can be utilized for impulse radar ranging or in ultra-wideband communication systems [42]. So the emergence of compact pulse-like signal voltages in NLTLs with interesting properties (no interactions, compactness and pulse width independent of the amplitude) can be used in the improvement of practical results concerning the above systems and the distortionless signal in high-speed signal processing systems. This work may inspire other researches on optical compact solitons in optical fibre cables which are of particular technological significance since the light-wave compact solitons can carry a large amount of digital information in long-distance communication. Similarly, since the nonlinear diffusive equation is usually used to describe contour detection and for nonlinear filtering of images, it will be very interesting to examine the role of compact structures for this application.

ACKNOWLEDGMENT

D. Yemélé would like to express deep gratitude to Professor Jean Marie Bilbault for helpful discussions during his recent visit in the LE2I Lab of the University of Bourgogne. The financial support of this Lab and the hospitality of the staff have been well appreciated.

REFERENCES

1. Rosenau, P. and J. M. Hyman, "Compactons: Solitons with finites wavelength," *Phys. Rev. Lett.*, Vol. 70, 564–567, 1993.
2. Remoissenet, M., *Waves Called Solitons*, 3rd Edition, Springer-Verlag, Berlin, 1999.
3. Rosenau, P. and E. Kashdan, "Compactification of nonlinear patterns and waves," *Phys. Rev. Lett.*, Vol. 101, 264101–264105, 2008.
4. Destrade, M., G. Gaeta, and G. Saccomandi, "Weierstrasss criterion and compact solitary waves," *Phys. Rev. E*, Vol. 75, 047601–047605, 2007.
5. Gaeta, G., T. Gramchev, and S. Walcher, "Compact solitary

waves in linearly elastic chains with non-smooth on-site potential," *J. Phys. A: Math. Theor.*, Vol. 40, 4493–4509, 2007.

6. Rosenau, P., "On compactification of patterns by a singular convection or stress," *Phys. Rev. Lett.*, Vol. 99, 234102–234107, 2007.
7. Kivshar, Y. S., "Intrinsic localized modes as solitons with a compact support," *Phys. Rev. E*, Vol. 48, 43–45, 1993.
8. Kevrekidis, P. G., V. V. Konotop, A. R. Bishop, and S. Takeno, "Discrete compactons: Some exact resuts," *J. Phys. A: Math. Gen.*, Vol. 35, 641–652, 2002.
9. Dusuel, S., P. Michaux, and M. Remoissenet, "From kinks to compacton like kinks," *Phys. Rev. E*, Vol. 57, 2320–2326, 1998.
10. Ludu, A. and J. P. Draayer, "Patterns on liquid surfaces cnoidal waves, compactons and scaling," *Physica D*, Vol. 123, 82–91, 1998.
11. Grimshaw, R. H. J., L. A. Ostrovsky, V. I. Shrira, and Y. A. Stepanyants, "Long nonlinear surface and internal gravity waves in a rotating ocean," *Surv. Geophys.*, Vol. 19, 289–338, 1998.
12. Takeno, S., "Compacton-like modes in model DNA systems and their bearing on biological functioning," *Phys. Lett. A*, Vol. 339, 352–360, 2005.
13. Rosenau, P. and A. Pikovsky, "Phase compactons in chains of dispersively coupled oscillators," *Phys. Rev. Lett.*, Vol. 94, 174102–174106, 2005.
14. Pikovsky, A. and P. Rosenau, "Phase compactons," *Physica D*, Vol. 218, 56–69, 2006.
15. Takahashi, D. and J. Satsuma, "Explicit solutions of magma equation," *J. Phys. Soc. Jpn.*, Vol. 57, 417–421, 1988.
16. Simpson, G., M. I. Weinstein, and P. Rosenau, "On a hamiltonian PDE arising in magma dynamics," *Disc. and Cont. Dynamical Systems B*, Vol. 10, 903–924, 2008.
17. Gharakhili, F. G., M. Shahabadi, and M. Hakkak, "Bright and dark soliton generation in a left-handed nonlinear transmission line with series nonlinear capacitors," *Progress In Electromagnetics Research*, Vol. 96, 237–249, 2009.
18. Afshari, E., H. S. Bhat, A. Hajimiri, and J. E. Marsden, "Extremely wideband signal shaping using one and two dimensional nonuniform nonlinear line," *J. Appl. Phys.*, Vol. 99, 054901–054917, 2006.
19. Narahara, K. and M. Nakamura, "Compensation of polarization mode dispersion with electrical nonlinear transmission lines," *Jpn. J. Appl. Phys.*, Vol. 42, 6327–6334, 2003.

20. Narahara, K., "Coupled nonlinear transmission lines for doubling repetition rate of incident pulse streams," *Progress In Electromagnetics Research Letters*, Vol. 16, 69–78, 2010.
21. Narahara, K., "Characterization of partially nonlinear transmission lines for ultrashort-pulse amplification," *Jpn. J. Appl. Phys.*, Vol. 42, 5508–5515, 2003.
22. Comte, J. C. and P. Marquié, "Compact-like kink in real electrical reaction-diffusion chain," *Chaos, Soliton, Fractals*, Vol. 29, 307–312, 2006.
23. Yemélé, D. and F. Kenmogné, "Compact envelope dark solitary wave in a discrete nonlinear electrical transmission line," *Phys. Lett. A*, Vol. 373, 3801–3809, 2009.
24. Kenmogné, F. and D. Yemélé, "Exotic modulated signals in a nonlinear electrical transmission line: Modulated peak solitary wave and gray compacton," *Chaos, Solitons, Fractals*, Vol. 45, 21–34, 2012.
25. English, L. Q., R. Basu Thakur, and R. Stearrett, "Patterns of travelling intrinsic localized modes in a driven electrical lattice," *Phys. Rev. E*, Vol. 77, 066601–066605, 2008.
26. Marquié, P., S. Binczak, J. C. Comte, B. Michaux, and J. M. Bilbault, "Diffusion effects in a nonlinear electrical lattice," *Phys. Rev. E*, Vol. 57, 6075–6078, 1998.
27. Comte, J. C., P. Marquié, J. M. Bilbault, and S. Binczak, "Noise removal using a nonlinear two-dimensional diffusion network," *Ann. Telecommun.*, Vol. 53, 483–487, 1998.
28. Nguena, H. K., S. Noubissi, and P. Woafo, "Waves amplification in nonlinear transmission lines using negative nonlinear resistance," *J. Phys. Soc. Jpn.*, Vol. 73, 1147–1150, 2004.
29. Ndzana, F., A. Mohamadou, and T. C. Kofané, "Modulated waves and chaotic-like behaviours in the discrete electrical line," *J. Phys. D: Appl. Phys.*, Vol. 40, 3254–3262, 2007.
30. Binzak, S., J. C. Comte, B. Michaux, P. Marquié, and J. M. Bilbault, "Experimental nonlinear electrical reaction-diffusion lattice," *Electron. Lett.*, Vol. 34, 1061–1062, 1998.
31. Saccomandi, G. and I. Sgura, "The relevance of nonlinear stacking interactions in simple models of double-stranded DNA," *J. R. Soc. Interface*, Vol. 3, 655–667, 2006.
32. Nguetcho, A. S., J. R. Bogning, D. Yemélé, and T. C. Kofané, "Kink compactons in models with parametrized periodic double-well and asymmetric substrate potentials," *Chaos, Solitons, Fractals*, Vol. 21, 165–176, 2004.

33. Rus, F. and F. R. Villatoro, "A repository of equation with cosine/sine compacton," *Appl. Math. Comput.*, Vol. 215, 1838–1851, 2009.
34. Burgers, J. M., *The Nonlinear Diffusion Equation: Asymptotic Solutions and Statistical Problems*, D. Reidel, Dordrecht-H, Boston, 1974.
35. Rosenau, P., "Nonlinear dispersion and compact structures," *Phys. Rev. Lett.*, Vol. 73, 1737–1741, 1994.
36. Rosenau, P., "On solitons, compactons and Lagrange maps," *Phys. Lett. A*, Vol. 211, 265–275, 1996.
37. Rosenau, P., "On nonanalytic solitary waves due to nonlinear dispersion," *Phys. Lett. A*, Vol. 230, 305–318, 1997.
38. Cooper, F., H. Shepard, and P. Sodano, "Solitary waves in a class of generalized KdV. equations," *Phys. Rev. E*, Vol. 48, 4027–4032, 1993.
39. Tanaka, M., "Perturbations on the KdV solitons an approach based on the multiple time scale expansion," *J. Phys. Soc. Jpn.*, Vol. 49, 807–812, 1980.
40. Rus, F. and F. R. Villatoro, "Diabatic perturbation for compactons under dissipation and numerically-induced dissipation," *J. Comput. Phys.*, Vol. 228, 4291–4302, 2009.
41. Kenmogné, F., D. Yemélé, and P. Woafo, "Electrical dark compacton generator: Theory and simulations," *Phys. Rev. E*, Vol. 85, 056606–056619, 2012.
42. Li, X., D. S. Ricketts and D. Ham, "Solitons in electrical networks," *McGraw-Hill 2008 Yearbook of Science and Technology*, 2008.